

# Blends of canal surfaces from polyhedral medial transform representations

Bohumír Bastl  
University of West Bohemia, Plzeň  
bastl@kma.zcu.cz

Miroslav Lávička  
University of West Bohemia, Plzeň  
lavicka@kma.zcu.cz

Bert Jüttler  
Johannes Kepler University of Linz  
bert.juettler@jku.at

Tino Schulz  
Johannes Kepler University of Linz  
tino.schulz@jku.at

## Abstract

We present a new method for constructing  $G^1$  blending surfaces between an arbitrary number of canal surfaces. The topological relation of the canal surfaces is specified via a convex polyhedron and the design technique is based on a generalization of the medial surface transform. The resulting blend surface consists of trimmed envelopes of one- and two-parameter families of spheres. Blending the medial surface transform instead of the surface itself is shown to be a powerful and elegant approach for blend surface generation. The performance of our approach is demonstrated by several examples.

## 1 Introduction

*Blending* is an important operation in any geometric modeling system. Given a number of surfaces, which are often called primary surfaces, the purpose of blending is to generate one or more auxiliary (secondary) surfaces that create a smooth transition between the primary ones. The final object then consists of trimmed primary surfaces and the auxiliary ones.

Blending surfaces are needed for rounding edges and corners of mechanical parts, or for smoothly joining separated objects. Some types of blend surfaces (which require the addition of material to an existing object) are called *fillets*, but there seems to be no universally accepted terminology.

Many engineering objects consists mostly of simple surfaces (segments of planes, cylinders, cones, tori and spheres) except for the blending surfaces, which require true free-form surfaces. Thus, blend surface creation is often the first challenge where it is necessary to introduce free-form design tools into a geometric modeling system.

Due to its technical importance, blending has continuously attracted the geometric design community since many years. Detailed introductions with any related references are provided in the two books [5, 12].

The existing approaches to blending can be classified according to the type of surfaces which are used to describe the blend surface. The rolling ball blend (see e.g. [17] and the references cited therein), which probably represents the earliest existing method, uses a *procedural description of the blend surface*. In its simplest form, a ball of constant radius rolls on two primary surfaces, thereby creating the blend surface as its envelope. The blend then

consists of segments of pipe surfaces which are, however, often approximated by other surfaces [6]. A generalization leads to variable radius rolling ball blends, consisting of segments of canal surfaces [2]. A new method for controlling the radius of a rolling ball blend has been proposed recently in [34].

*Parametric blend surfaces* are often favored in applications, since they can easily be added to an existing boundary representation of a solid using trimmed surfaces. These blending surfaces can be defined by specifying contact curves on the given primary surfaces and then creating a blend surface that is smoothly joined to the given surfaces. In 1994, a survey of blending methods of this type was presented by Vida et al. [31]. The special case of parametric blending surfaces between pairs of quadric surfaces was addressed in [32].

Recent results on parametric blend surfaces include the article [28], which uses a partial reparameterization of the base surfaces, as well as techniques for blending subdivision surfaces [13].

When using parametric blend surfaces, however, the flexibility of these surfaces is rather limited, since the mathematical description of these surfaces requires to define them as embeddings of a parameter domain. While this works well for blends between only two surfaces, the description of multi-sided blends (e.g. the house-corner blend, which requires a six-sided surface) is not that obvious. Consequently, special techniques for the construction of vertex blends have been designed [30, 38]. In a recent paper, surfaces defined in polar coordinates were used to define blends between multiple surfaces and to fill  $n$ -sided holes [26].

In order to optimize the shape of blend surfaces, numerical methods for solving geometric partial differential equations have been studied in [36].

On the other hand, the use of *implicitly defined blend surfaces* offers more flexibility for designing blends, since their shape is not restricted to be obtained as an embedding of a parameter domain. Due to this flexible topology, it is easier to obtain complex, multi-sided blends. The classical texts on use of implicit surfaces for blending include [10] and [33]. Since then, blending using implicit representations has been discussed by a large number of authors. We refer to [7, 8, 35, 39, 4, 18] as a few representative references. Besides blends based on (piecewise) polynomial representations, also procedurally defined implicit representations were used to create blends [9].

Another possibility to classify blending surfaces is to analyze the class of primary surfaces that can be dealt with. Here, special attention has been paid to blending surfaces between *canal surfaces* and more generally, of ringed surfaces. In particular, it has been proposed to use patches of Dupin cyclides as blends between canal surfaces; see the chapter on cyclides in [5].

These cyclides can be defined as the envelopes of all spheres that touch three given spheres; see [3]. They are algebraic surfaces of degree four and they possess simple rational parameterizations with the parameter lines being simultaneously lines of curvature. Moreover, the class of Dupin cyclides is closed under offsetting. Cyclide blends between two cones were analyzed in [25]. By generalizing the constructions of biarcs to Laguerre geometry it was shown how to generate blends between general canal surfaces using double-cyclide surfaces in [24].

In a recent paper, Krasauskas [15] creates *branching blends* of natural quadrics that are also surfaces with rational offsets. These blend surfaces are defined as envelopes of special two-parameter families of planes.

We present a new approach to create blend surfaces between an arbitrary number of canal surfaces, which also covers the case of branching blends discussed by Krasauskas. Our approach is based on the use of a *medial structure*. Recall that the medial axis representation

of a solid allows to represent its boundary as the envelope of two- and one-parameter families of spheres, which correspond to the sheets and to the seams of the medial axis, respectively. These spheres are the boundaries of the maximum inscribed balls (with respect to inclusion) of the given solid object. The medial structures has become a popular research area in recent years – mathematicians have studied the properties of these representations, and computer scientists and engineers have developed a variety of algorithms for computing and using these models; cf. [27] and references therein for a detailed survey of this topic.

In addition to the use of the medial axis, which turns out to be too stiff for the design of blending surfaces in certain situations, we propose to design blend surfaces using a *polyhedral medial structure*. This structure again consists of sheets and seams representing centers and radii of inscribed balls. As the main difference to the medial axis, however, these balls are not required to be maximal, but only to touch the boundary in at least one point. If such a medial structure is given, then it is possible to recover the boundary of the object – and hence the blend surface – as envelopes of certain one- and two-parameter families of spheres. Not all branches of these envelopes then contribute to the blend. By adding constants to the (non-constant) function specifying the radius of these balls it is possible to obtain the offsets of the blend surfaces.

The remainder of this paper is organized as follows. The next section summarizes several fundamental facts concerning the representation of one- and two parameter families as curves and surfaces in the Minkowski space  $\mathbb{R}^{3,1}$ . Section 3 introduces the polyhedral medial transform representation which serves as the tool to create blends between canal surfaces. The details of the construction of single-sheeted and polyhedral blends will be presented in Sections 4 and 5, respectively. After presenting several examples, which illustrate the capabilities of our method, we conclude this paper.

## 2 Preliminaries

In this section we briefly summarize some fundamental notions and basic properties of the four-dimensional Minkowski space  $\mathbb{R}^{3,1}$  and the medial axis/surface (MA/MS) and medial axis/surface transform (MAT/MST) representations.

### 2.1 Minkowski space $\mathbb{R}^{3,1}$

The *Minkowski space*  $\mathbb{R}^{3,1}$  is a four-dimensional real affine space which is equipped with the indefinite inner product

$$\langle \mathbf{u}, \mathbf{v} \rangle = \mathbf{u}^\top \mathbf{J} \mathbf{v} = u_1 v_1 + u_2 v_2 + u_3 v_3 - u_4 v_4 \quad (1)$$

defined by the diagonal matrix

$$\mathbf{J} = (\mathbf{J}_{i,j})_{i,j=1,2,3,4} = \text{diag}(1, 1, 1, -1), \quad (2)$$

where  $\mathbf{u} = (u_1, u_2, u_3, u_4)^\top$ ,  $\mathbf{v} = (v_1, v_2, v_3, v_4)^\top$ . The four axes spanned by the vectors  $(\delta_{i,1}, \delta_{i,2}, \delta_{i,3}, \delta_{i,4})^\top$ ,  $i = 1, \dots, 4$ , will be called the  $x$ -,  $y$ -,  $z$ - and  $r$ -axis, respectively.

The squared norm of a vector defined by  $\|\mathbf{v}\|^2 = \langle \mathbf{v}, \mathbf{v} \rangle$ , can be positive, negative or zero. We distinguish three types of vectors (and thus also of corresponding lines with these directions): *space-like* if  $\|\mathbf{v}\|^2 > 0$ , *time-like* if  $\|\mathbf{v}\|^2 < 0$ , and *light-like* (or *isotropic*) if  $\|\mathbf{v}\|^2 = 0$ . Analogously for  $d > 1$ , a  $d$ -dimensional linear subspace of  $\mathbb{R}^{3,1}$  is called *space-*,

*time-* or *light-like* if the restriction of the quadratic form defined by  $\mathbf{J}$  is positive definite, indefinite non-degenerate or degenerate, respectively.

Let  $\mathbf{a}$  be a point in  $\mathbb{R}^{3,1}$  and  $\hat{\mathbf{x}} = (X, Y, Z, 0)^\top$ . Then

$$\langle \hat{\mathbf{x}} - \mathbf{a}, \hat{\mathbf{x}} - \mathbf{a} \rangle = 0, \quad (3)$$

defines a sphere in  $\mathbb{R}^3$  centered at  $(a_1, a_2, a_3)^\top$  and with the oriented radius  $a_4$ . We recall that the correspondence between points in  $\mathbb{R}^{3,1}$  and oriented spheres in  $\mathbb{R}^3$  can be established via the so called *cyclographic mapping*; cf. [23, 24].

## 2.2 Curves in $\mathbb{R}^{3,1}$

Considering a curve  $\mathbf{c}(t) = (\hat{\mathbf{c}}(t), r(t))^\top \subset \mathbb{R}^{3,1}$ ,  $t \in I \subseteq \mathbb{R}$ , its points correspond to spheres whose centers trace the curve  $\hat{\mathbf{c}}(t)$  in  $\mathbb{R}^3$  and possess the radii  $r(t)$ . The envelope of this one-parameter family of spheres

$$\mathcal{F}(t) : \langle \hat{\mathbf{x}} - \mathbf{c}(t), \hat{\mathbf{x}} - \mathbf{c}(t) \rangle = 0 \quad (4)$$

is called a *canal surface* and the curve  $\hat{\mathbf{c}}(t)$  is called its *spine curve*. If  $r(t) = \text{const.}$ , we obtain a *pipe surface*. The defining equations for the canal surface  $\mathcal{C}$  are

$$\mathcal{F}(t) = 0, \quad \mathcal{F}'(t) = 0, \quad (5)$$

where  $\mathcal{F}'$  denotes the derivative with respect to  $t$ .

The equation  $\mathcal{F}'(t) = 0$  describes the plane perpendicular to the derivative vector  $\mathbf{c}'(t)$ . Thus the canal surface  $\mathcal{C}$  contains a one-parameter set of the so called *characteristic circles*  $\mathcal{F}(t) \cap \mathcal{F}'(t)$ . Note that for  $\mathbf{c}(t)$  being straight lines we obtain cylinders and cones.

The envelope of the one-parameter family of spheres may not be real, depending on the relation between  $\hat{\mathbf{c}}'(t)$  and  $r'(t)$ . More precisely, the envelope is real if  $\mathbf{c}'(t)$  is not time-like. In particular, if  $\mathbf{c}'(t)$  is light-like for a parameter value  $t_0$ , then the plane  $\mathcal{F}'(t_0) = 0$  is tangent to the sphere  $\mathcal{F}(t_0) = 0$  and the corresponding characteristic circle degenerates to a point.

Moreover, as proved in [22, 16], a canal surface given by a rational curve  $\mathbf{c}(t)$  possesses always a rational parameterization. However, it should be noted that the computation of a rational parameterization is still a challenging problem, which is equivalent to the SOS (sum of squares) problem for non-negative polynomials.

## 2.3 Surfaces in $\mathbb{R}^{3,1}$

Considering a surface  $\mathbf{s}(u, v) = (\hat{\mathbf{s}}(u, v), r(u, v))^\top \subset \mathbb{R}^{3,1}$ ,  $(u, v) \in I \subseteq \mathbb{R}^2$ , its points correspond to spheres whose centers trace the surface  $\hat{\mathbf{s}}(u, v)$  in  $\mathbb{R}^3$  and possess the radii  $r(u, v)$ . The envelope of this two-parameter family of spheres

$$\mathcal{F}(u, v) : \langle \hat{\mathbf{x}} - \mathbf{s}(u, v), \hat{\mathbf{x}} - \mathbf{s}(u, v) \rangle = 0 \quad (6)$$

is generally a surface in  $\mathbb{R}^3$ . The defining equations for the envelope surface  $\mathcal{B}$  are

$$\mathcal{F}(u, v) = 0, \quad \mathcal{F}_u(u, v) = 0, \quad \mathcal{F}_v(u, v) = 0, \quad (7)$$

where  $\mathcal{F}_u, \mathcal{F}_v$  denote the partial derivatives with respect to  $u, v$ , respectively. Solving (7) we arrive at the coordinates of a point  $\mathbf{b} = (X, Y, Z)^\top$  of the envelope surface  $\mathcal{B}$  described by the the closed-form *envelope formula* (cf. [14]) in the form

$$\mathbf{b}^\pm(u, v) = \hat{\mathbf{s}}(u, v) + \frac{r}{\hat{C}} \left( \mathbf{w} \pm \sqrt{C} \cdot (\hat{\mathbf{s}}_u \times \hat{\mathbf{s}}_v) \right), \quad (8)$$

where

$$\hat{C} = \hat{E}\hat{G} - \hat{F}^2, \quad C = EG - F^2. \quad (9)$$

The components  $E, F, G$  of the first fundamental form of  $\mathbf{s}(u, v)$  are computed using the Minkowski inner product in  $\mathbb{R}^{3,1}$ , whereas the components  $\hat{E}, \hat{F}, \hat{G}$  of the first fundamental form of  $\hat{\mathbf{s}}(u, v)$  are determined using the standard Euclidean inner product in  $\mathbb{R}^3$ . The vector  $\mathbf{w} = \mathbf{w}(u, v)$  in (8) consists of polynomials of degree four in  $x_u, y_u, z_u, r_u$  and  $x_v, y_v, z_v, r_v$ ; see [14] for more details. Clearly, the envelope is real if  $C \geq 0$ .

Unlike the case of canal surfaces, not all envelope surfaces given by rational  $\mathbf{s}(u, v)$  are rational. This was a motivation for introducing the so called MOS surfaces in [14]. The parameterization  $\mathbf{s}(u, v)$  is called an *MOS parameterization* if there exists a bivariate polynomial or rational function  $\sigma(u, v)$ , such that it holds

$$EG - F^2 = \sigma(u, v)^2. \quad (10)$$

Then, the surface in  $\mathbb{R}^{3,1}$  having an MOS parameterization is called an *MOS surface*.

A distinguishing property of MOS surfaces is that not only both branches of the envelope but also their offsets possess an exact rational parametric representation, i.e., the envelope surfaces belong to the class of the so called *surfaces with Pythagorean normals* (PN surfaces).

It has been recently proved in [21] that quadratic triangular Bézier surfaces in  $\mathbb{R}^{3,1}$  possess the MOS property. A related study followed in [20, 19] and an algorithm for computing boundaries and trimmed offsets of volumes given by piecewise quadratic medial surface transforms was designed and studied in [1]. As polynomial quadratic patches in  $\mathbb{R}^{3,1}$  are capable of producing  $C^1$  approximations to free-form surfaces considered as medial surface transforms, this algorithm can be also used for computing rational approximations of volume boundaries and all their offsets.

## 2.4 MA/MS and MAT/MST representations

Consider a spatial domain  $\Omega \subset \mathbb{R}^3$  with a smooth boundary. The *medial locus*, or *skeleton*, of this domain is constructed as the closure of the locus of all centers of maximal balls inscribed into  $\Omega$ . The local thickness of the object is measured by the radii  $r$  of these maximal balls.

Except in special cases, the medial locus is a two-dimensional *medial surface* (MS). Degeneracies occur only for spheres when the medial locus is a single point, or for the canal surfaces (e.g. cylinders, cones, Dupin cyclides) when the medial loci are their spine curves. Hence, in the case of canal surfaces we speak about *medial axis* (MA).

By appending the corresponding ball radii  $r$  to the points  $(x, y, z)^\top$  of the medial axis/surface MA/MS, we obtain the *medial axis/surface transform* MAT/MST consisting from points  $(x, y, z, r)^\top$ . Thus all maximal inscribed oriented balls, can be identified as the points in the four-dimensional Minkowski space  $\mathbb{R}^{3,1}$ .

In general, the medial surface transforms can consist of components of dimensions two, one, and zero, which are called *sheets*, *seams* and *junctions*, respectively. Their points correspond

to maximal inscribed balls which, generically, touch the boundary in two, three, and four points, respectively. The sheets meet in seams, and the seams meet in junctions.

Finally, let us emphasize that when starting from the medial surface/axis transform as a shape representation, one has to guarantee that the associated domain boundary is a *valid boundary* (real, without self-intersections, etc.). More details about the validity of MATs/MSTs can be found e.g. in [11, 29, 37].

### 3 Polyhedral medial transform representation

In this section we will introduce the notion of a *polyhedral medial transform (MT) representation*, which we will use later for the construction of blend surfaces.

Recall that the medial surface transform of a domain  $\Omega \subset \mathbb{R}^3$  with a piecewise smooth boundary generically consists of several components with different dimensions. Moreover, if the medial surface transform is known it is possible to completely reconstruct the corresponding domain.

Instead of using the medial axis as a representation of shape, we consider shapes that can be reconstructed from a different, more general medial representation. Let  $\mathbf{P} \subset \mathbb{R}^3$  be a convex polyhedron with  $d \geq 2$  faces and boundary surface  $\partial\mathbf{P}$ . A set  $\mathbf{Q} \subset \mathbb{R}^{3,1}$  is called a *polyhedral medial transform (MT) with shape  $\mathbf{P}$*  if the following conditions are satisfied:

1.  $\mathbf{Q}$  is homeomorphic to  $\mathbf{P}$ .
2. There exists a continuous, piecewise smooth mapping  $\mathbf{F} : \partial\mathbf{P} \rightarrow \partial\mathbf{Q}$  that is regular and smooth in the interior of each face of  $\mathbf{P}$  and with the property that all edges are mapped to regular curves.
3. For each face  $f \subset \partial\mathbf{P}$ , all points on  $\mathbf{F}(f)$  (also on boundaries and vertices) possess a well defined tangent plane (the limit of the tangent planes, when we go to the vertex, is unique).
4. All edges and vertices of  $\mathbf{Q}$  are strictly convex.
5. The radius (i.e., the fourth coordinate of  $\mathbf{Q}$ ) is strictly positive

The boundary  $\partial\mathbf{Q}$  of a polyhedral medial transform  $\mathbf{Q}$  consists of a collection of  $d$  smooth surfaces. Each of these surfaces corresponds to exactly one face of  $\mathbf{P}$  and their mutual adjacency relation is inherited from  $\mathbf{P}$ . One may think of  $\mathbf{Q}$  as a feature-preserving distortion of  $\mathbf{P}$ , embedded in  $\mathbb{R}^{3,1}$ .

Note that the mapping  $\mathbf{F}$  which is required to exist in (ii) is only assumed to be regular and smooth in the *interior* of each face, hence the images of the faces can be patches with singular vertices. Later we will use this possibility to define blend surfaces. Nevertheless, (iii) guarantees that these patches possess a well-defined tangent plane everywhere.

A domain  $\Omega \subset \mathbb{R}^3$  is said to possess a *polyhedral MT representation of shape  $\mathbf{P}$* , if its boundary  $\partial\Omega$  can be reconstructed from a polyhedral medial transform with shape  $\mathbf{P}$ , i.e., if there exists a polyhedral medial transform  $\mathbf{Q}$  such that for

$$\hat{\Omega} = \pi(\mathbf{Q}) \cup \bigcup_{\mathbf{q} \in \partial\mathbf{Q}} \{\mathbf{x} \in \mathbb{R}^3, \|(\mathbf{x}, 0)^\top - \mathbf{q}\| = 0\} \quad (11)$$

with  $\pi : \mathbb{R}^{3,1} \rightarrow \mathbb{R}^3, (\mathbf{x}, r) \mapsto \mathbf{x}$  we have  $\partial\Omega \subset \partial\hat{\Omega}$ .

Note that the norm  $\|\cdot\|$  is measured in  $\mathbb{R}^{3,1}$ , hence the second part of this formula contributes the points on the boundaries of all spheres represented by points on the boundary  $\partial\mathbf{Q}$ . The first part  $\pi(\mathbf{Q})$  was added in order to avoid inner boundaries that might appear otherwise.

A very simple example with a medial tetrahedron is shown in Fig. 1. The boundary of the associated solid consists of six pieces of canal surfaces, which correspond to the edges, four spherical segments, which correspond to the vertices, and four surface patches, which correspond to the faces of the polyhedron. More precisely, the surface patches are planes and the canal surfaces are cones and cylinders of revolution.

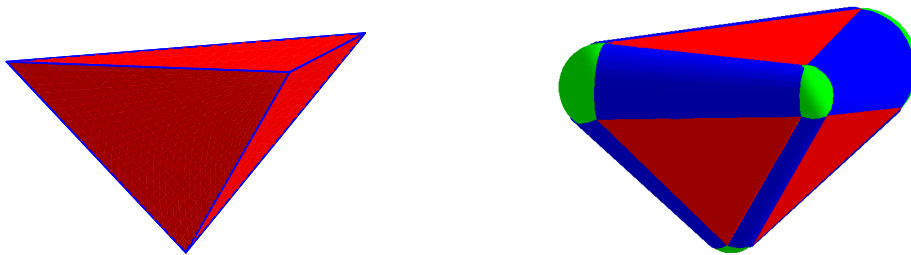


Figure 1: The projection  $\pi(\mathbf{Q})$  of a polyhedral medial transform (left) and the reconstructed domain  $\Omega$  (right).

In general, if the values of the radius function are sufficiently small, a domain with a polyhedral MT representation of shape  $\mathbf{P}$  will be bounded by a collection of pieces of spheres, trimmed canal surfaces and generalized, one-sided offsets. Moreover, in that case, the numbers of spheres, canal surfaces and generalized offsets match the numbers of vertices, edges and faces of  $\mathbf{P}$ , respectively.

In the special case  $d = 2$ , the polyhedron  $\mathbf{P}$  degenerates into a planar polygon. The two boundary surfaces of  $\mathbf{Q}$  will be equal to each other as well as equal to the medial axis (or surface) transform of  $\Omega$ . *Thus, in this situation, the polyhedral MT representation becomes the usual medial transform representation.*

We will now use medial polyhedrons to design blends between several canal surfaces.

## 4 Single-sheeted blends of canal surfaces

In this section we will focus on single-sheeted blends which are nothing else than special cases of the polyhedral ones, where the medial polyhedron degenerates into a single face. For more details about the mathematical properties of the medial representations and the relation between it and the corresponding domain boundary see [27].

We start with blending of three canal surfaces represented by their spine curves and associated radii. Subsequently, we modify this design approach to generate branching blends and general case of  $n$ -way blends.

As the envelope of a one-parameter family of spheres can be also generated as the envelope of a one-parameter family of cones/cylinders of revolution (cf. [23]) we can reduce studying the blends of canal surfaces to simpler input primitives, i.e., to cones and cylinders.

#### 4.1 Three curves

We consider three canal surfaces  $\mathcal{C}_1, \mathcal{C}_2, \mathcal{C}_3$  represented by their MATs  $\mathbf{c}_1, \mathbf{c}_2, \mathbf{c}_3$  in  $\mathbb{R}^{3,1}$ . The polyhedral medial surface transform representing a single-sheeted blend can be then constructed by the following three steps:

1. Determine three points  $\mathbf{p}_1, \mathbf{p}_2, \mathbf{p}_3$  representing end characteristic circles and associated three directional vectors  $\mathbf{t}_1, \mathbf{t}_2, \mathbf{t}_3$  at these points from MATs  $\mathbf{c}_1, \mathbf{c}_2, \mathbf{c}_3$ , which are data describing the  $G^1$  join.
2. Construct a suitable Bézier triangle patch  $\mathbf{Q}$  in  $\mathbb{R}^{3,1}$  interpolating the given data.
3. Find the associated  $\partial\Omega$ .

Steps (i) and (iii) are straightforward. Hence, we describe only Step (ii) in more detail.

*Step (ii):* We construct a Bézier triangle patch of degree five, which is the smallest possible degree of the patch to fulfill the necessary conditions.

(a) *Initialization:*

The corner control points of the constructed patch are directly the input points, i.e.,  $\mathbf{b}_{500} = \mathbf{p}_1, \mathbf{b}_{050} = \mathbf{p}_2, \mathbf{b}_{005} = \mathbf{p}_3$ . Both neighboring control points of  $\mathbf{p}_i$  have to lie on the line determined by  $\mathbf{p}_i$  and  $\mathbf{t}_i$ . Further, to have a well-defined tangent plane also at a singularly parametrized corner point, the control points  $\mathbf{b}_\alpha, \alpha = (ijk) \in \{(311), (131), (113)\}$ , have to satisfy a certain linear condition.

(b) *Boundary optimization:*

We use the second order differences of control points, i.e.,  $\mathbf{b}_\alpha - 2\mathbf{b}_{\alpha+1} + \mathbf{b}_{\alpha+2}$ . We choose this method in order to maintain cylinders/cones and to minimize the curvature along the boundary.

(c) *Optimization of interior control points:*

The remaining points are determined by minimizing the sum of the squared distances of neighboring control points.

Clearly, one might consider other things to minimize in step (b), such as curvature variation. However, this may not reproduce cylinders and cones.

Fig. 2 shows an example of a 3-way blend (bottom) along with the corresponding polyhedral medial structure (top). The blend surface connects three given cylinders with different radii and non-intersecting axes. It consists of two generalized offset surfaces (red) and three canal surfaces (blue) which correspond to the edges and faces of the medial structure.

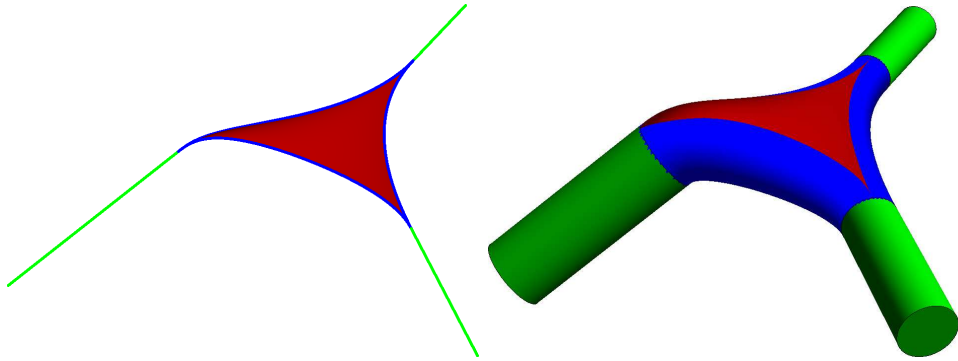


Figure 2: Example of a 3-way blend.

#### 4.2 Two curve branching

The designed method from the previous subsection can be immediately used also for the construction of branching blends. This is guaranteed by using the boundary optimization in Step (ii) which enables to preserve the shape of cylinders/cones.

A series of examples is shown in Fig. 3. We visualize several branching blends between two given cylinders. The construction of the medial surface reproduces lines as boundary curves, hence it automatically preserves the bigger cylinder, creating the desired branching blend.

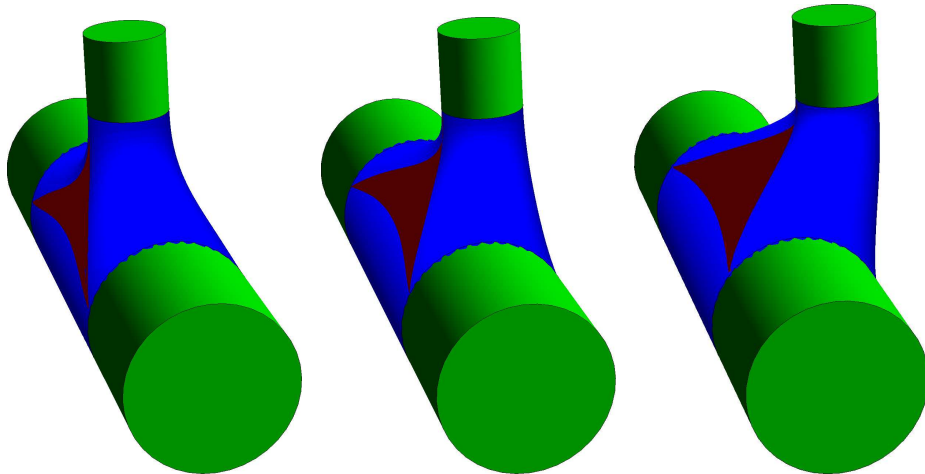


Figure 3: Examples of 3-way blends used for obtaining branching blends.

#### 4.3 Free $n$ -way blend

Finally we describe a construction of an  $n$ -way blend. If not just three, but  $n > 3$  cylinders/cones  $\mathcal{C}_i$  with prescribed end circles are given, a blend surface can be generated by replacing the Bézier triangle in Step (ii) with a suitable  $n$ -sided patch.

We demonstrate this for  $n = 4$  on several examples, cf. Fig. 4–6 which show two different blends between four cylinders and two cones.

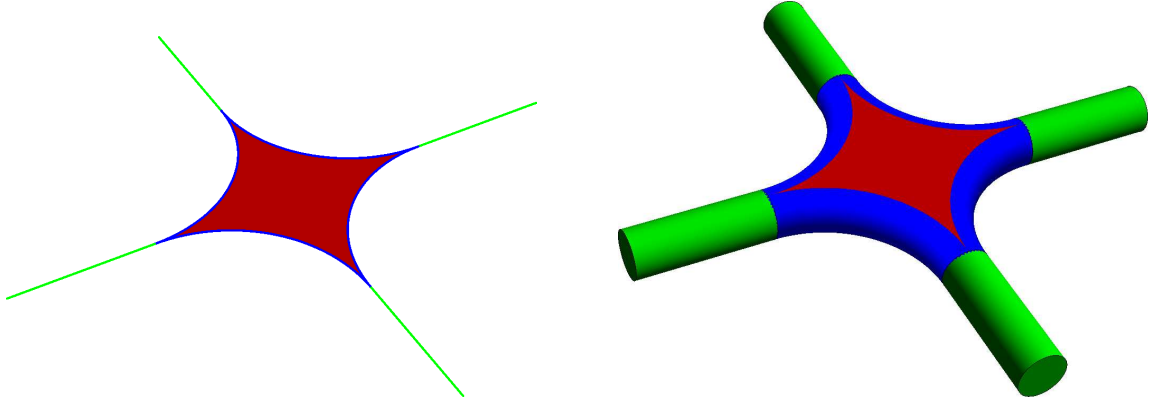


Figure 4: 4-way blend of two cylinders

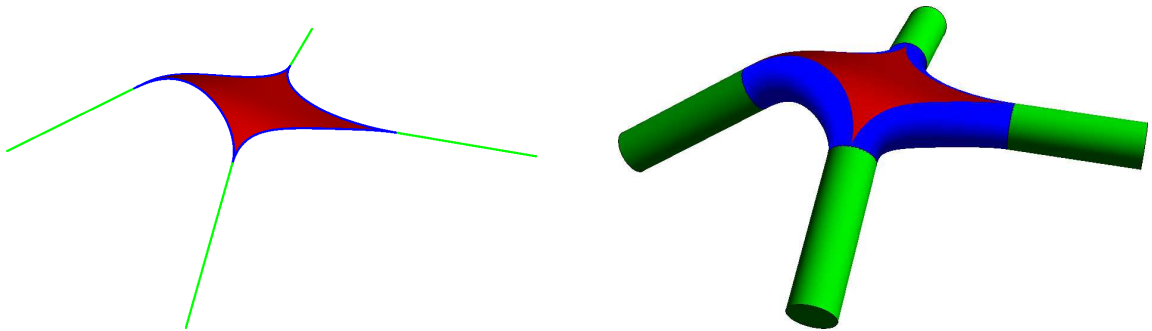


Figure 5: Examples of 4-way blend of two cylinders

In the last example, the single-sheeted blend does not preserve the two cones, since none of them corresponds to an edge of the four-sided medial surface.

The situation is different in the next example, which is shown in Fig. 7. Here, the two given cylinders correspond to two of the four edges of the medial surface, thereby creating a blend surface which preserves cylinders/cones. The shape of the blend, however, is not really satisfying and becomes even worse when the angle between the cylinders approaches 90 degrees. In this situation it is more appropriate to use polyhedral blends.

## 5 Polyhedral blends

Although the single-sheeted blend is rather elegant and flexible, it still possesses certain limitations. Due to its construction, every canal surface must have exactly two adjacent canal surfaces. Thus even for certain relatively simple configurations, e.g. the one shown in Fig. 7, the shape of the obtained blend surface is different from the shape one would expect.

However, other configurations of canal surfaces may be blended properly by constructing medial polyhedra with more faces. For blending  $n$  canal surfaces, like in Section 4, one

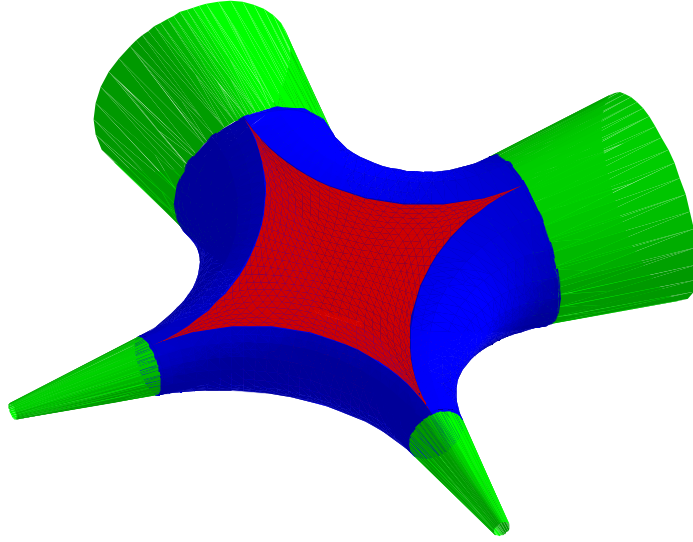


Figure 6: Single-sheeted four way blend of two cones with coplanar axes

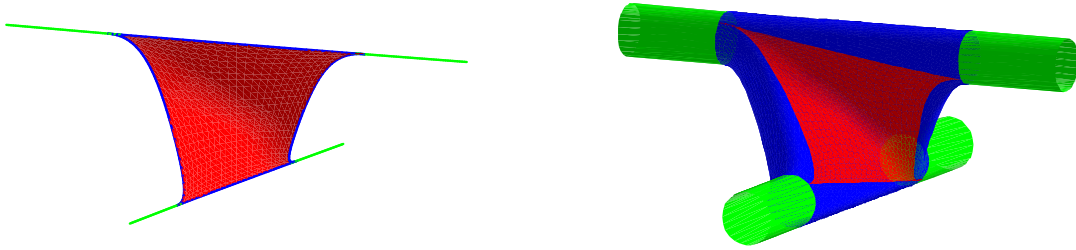


Figure 7: Single-sheeted four way blend of two skew cylinders.

picks a convex polyhedron  $\mathbf{P}$  that reflects the topological structure of the canal surfaces: characteristic circles correspond to vertices and a polynomial canal surface corresponds to an edge, including its two vertices. Again, a one-to-one correspondence between vertices and characteristic circles is needed.

For each face of  $\mathbf{P}$  we can now apply the single-sheeted algorithm from the previous section to obtain the complete medial polyhedron. Adjacent patches will necessarily have common boundary curves, since the optimization of each singular boundary curve only depends on the two given points and tangents it connects.

Thus the construction of complex medial polyhedrons can be completely reduced to the construction of single-sheeted medial polyhedrons. Of course, the trimming of the constructed boundary surface needs to be modified, but however, the amount of reasonably treatable configurations is greatly enhanced. In Table 5 the whole construction process is summarized.

In the following we will present some examples to illustrate the usefulness of this approach.

**Blending  $n$  canal surfaces with MATs  $\mathbf{c}_1, \dots, \mathbf{c}_n \in \mathbb{R}^{3,1}$** 

1. Determine  $n$  points  $\mathbf{p}_1, \dots, \mathbf{p}_n$  representing the characteristic circles and associated directional vectors  $\mathbf{t}_1, \dots, \mathbf{t}_n$  at these points from MATs  $\mathbf{c}_1, \dots, \mathbf{c}_n$ , which are data describing the  $G^1$  join.
2. Choose a convex polyhedra  $\mathbf{P}$  with  $n$  vertices, specifying the topological relation of the canal surfaces. Each vertex corresponds to exactly one characteristic circle.
3. For each edge of  $\mathbf{P}$ , find a quintic Bézier curve in  $\mathbb{R}^{3,1}$  that interpolates the points and direction vectors corresponding to the vertices of the edge. Specify its control points by minimizing the sum of squared second order differences in between them.
4. For each face of  $\mathbf{P}$ , find a multi-sided surface patch in  $\mathbb{R}^{3,1}$  that interpolates the Bézier curves corresponding to the edges of the face and possesses well-defined tangent planes at its vertices. For a three- or foursided Bézier surface patch, specify its control points by minimizing the sum of squared distances in between them.
5. Find the associated boundary, i.e., the blend surface, by computing and trimming the envelopes of the one- and two-parameter families of spheres that correspond to the constructed curves and surfaces.

Table 1: Summary of the blend construction

**5.1 Tetrahedral blend**

This first example was motivated by the fact that with a single-sheeted approach, one is not able to yield a reasonable blending surface of two close or even intersecting, non-parallel cylinders. Except for the case that the axes of the two cylinders intersect, the single-sheeted approach always produces either a non-symmetric or a non-interpolating blend.

By choosing a tetrahedron instead of a four-sided patch, we are able to create a reasonable and symmetric blend. Therefore we identified the given cylinders with two skew edges of the tetrahedron.

Fig. 8 shows an example of such a tetrahedral blend between two partially intersecting cylinders. The upper picture shows the projection  $\pi(\mathbf{Q})$  of the polyhedral MT and the final blend – which consists of six trimmed canal surfaces (including the cylinders) and four one-sided, generalized offsets – is shown in the lower part.

**5.2 Cubical blend**

Naturally, there is a configuration where a multi-sheeted approach turns out to be more suitable: blending multiple canal surfaces whose tangents at the endpoints are far away from being in one plane.

Fig. 9 shows a polyhedral blending of eight cylinders, having their axes equally distributed in space. All cylinder axes intersect in one point and the final blend surface (bottom) consists of twelve trimmed canal surfaces and six generalized, one-side offsets.

### 5.3 Pyramidal blend

As a final example we consider a cylinder which splits up into four cones. The defining convex polyhedron is a square pyramid and the cylinder corresponds to the apex (cf. Fig. 10). The medial polyhedron consists of four triangular patches and one additional quadrilateral surface patch.

## 6 Conclusion

We presented a simple but powerful method for creating blend surfaces between an arbitrary number of canal surfaces. Our approach is based on a medial structure which can be seen as a generalization of the medial axis/medial surface transform of a solid object. By preserving existing canal surfaces, our approach can also be used to generate branching blends. The blend surfaces consist of canal surfaces and generalized offsets, which correspond to the edges and the faces of the medial transform structure, respectively.

There are several questions associated with our construction that deserve additional investigations.

The first one concerns the regularity of the generated blend surfaces. It is relatively simple to use the existing conditions to analyze a posteriori the regularity of the blend surfaces. However, it would be more desirable to find sufficient conditions on the shape of the given canal surfaces that guarantee regularity.

The second question is related to the parameterization of the obtained blend surfaces. Currently, we generate parameterizations that involve square-root functions. Thus, an approximation step is required in order to convert them into the accepted NURBS format. An approximation of the medial transform representation, e.g., by piecewise quadratic patches, would allow us to use the techniques for exact parameterizations of the envelopes developed in [1].

Finally, the construction is currently limited to  $G^1$  smooth blend surfaces. The construction of blends with higher order of smoothness requires additional conditions on the medial transform representations. It would be interesting to analyze them and to see how they can be used for designing shapes.

**Acknowledgments** B. Bastl and M. Lávička have been supported by Research Plan MSM 4977751301. B. Jüttler and T. Schulz have been supported by the Austrian Science fund, project S9202. All authors were supported by the Austrian/Czech AKTION 2009/5 (MEB060905).

## References

- [1] B. Bastl, B. Jüttler, J. Kosinka, and M. Lávička. Volumes with piecewise quadratic medial surface transforms: Computation of boundaries and trimmed offsets. *Computer-Aided Design*, 42(6):571–579, 2010.
- [2] J. Chuang and W. Hwang. Variable-radius blending by constrained spine generation. *The Visual Computer*, 13(7):316–329, 1997.
- [3] D. Dutta, R. R. Martin, and M. J. Pratt. Cyclides in surface and solid modeling. *IEEE Computer Graphics and its Applications*, 13:53–59, 1993.
- [4] M. Fang, G. Wang, and W. Ma. N-way blending problem of circular quadrics. *SCIENCE CHINA Information Sciences*, 53(8):1546–1554, 2010.
- [5] G. Farin and J. Hoschek. *Handbook of computer aided geometric design*. North Holland, 2002.

- [6] R. Farouki and R. Sverrison. Approximation of rolling-ball blends for free-form parametric surfaces. *Computer-Aided Design*, 28:871–878, 1996.
- [7] E. Hartmann. Blending of implicit surfaces with functional splines. *Computer-Aided Design*, 1990.
- [8] E. Hartmann.  $G^n$ -continuous connections between normal ringed surfaces. *Computer aided geometric design*, 18(8):751–770, 2001.
- [9] E. Hartmann. Parametric  $G^n$  blending of curves and surfaces. *The Visual Computer*, 17(1):1–13, 2001.
- [10] C. Hoffmann and J. Hopcroft. The Potential Method for Blending Surfaces and Corners. In G. Farin, editor, *Geometric modeling: Algorithms and new trends*, pages 347–365. SIAM, 1987.
- [11] C. M. Hoffmann and P. J. Vermeer. Validity determination for MAT surface representation. In *Proceedings of the 6th IMA Conference on the Mathematics of Surfaces*, pages 249–265, New York, NY, USA, 1996. Clarendon Press.
- [12] J. Hoschek and D. Lasser. *Fundamentals of computer-aided geometric design*. AK Peters, 1993.
- [13] K. Hui and Y. Lai. Smooth blending of subdivision surfaces. *Computer-Aided design*, 38:786–799, 2006.
- [14] J. Kosinka and B. Jüttler. MOS surfaces: Medial surface transforms with rational domain boundaries. In *The Mathematics of Surfaces XII*, volume 4647 of *Lecture Notes in Computer Science*, pages 245–262. Springer, 2007.
- [15] R. Krasauskas. Branching blend of natural quadrics based on surfaces with rational offsets. *Computer Aided Geometric Design*, 25(4-5):332–341, 2008.
- [16] G. Landsmann, J. Schicho, and F. Winkler. The parametrization of canal surfaces and the decomposition of polynomials into a sum of two squares. *Journal of Symbolic Computation*, 32(1-2):119 – 132, 2001.
- [17] G. Lukacs. Differential geometry of  $G^1$  variable radius rolling ball blend surfaces. *Computer-Aided Geometric Design*, 15:585–613, 1998.
- [18] H. Mou, G. Zhao, Z. Wang, and Z. Su. Simultaneous blending of convex polyhedra by algebraic splines. *Computer-Aided Design*, 39(11):1003–1011, 2007.
- [19] M. Peternell. Rational two-parameter families of spheres and rational offset surfaces. *Journal of Symbolic Computation*, 45(1):1–18, 2010.
- [20] M. Peternell and B. Odehnal. On generalized LN-surfaces in 4-space. In *Proceedings of 'ISSAC08'*, pages 223–230, 2008.
- [21] M. Peternell, B. Odehnal, and M. Sampoli. On quadratic two-parameter families of spheres and their envelopes. *Computer Aided Geometric Design*, 25:342–355, 2008.
- [22] M. Peternell and H. Pottmann. Computing rational parametrizations of canal surfaces. *J. Symb. Comput.*, 23:255–266, February 1997.
- [23] M. Peternell and H. Pottmann. A Laguerre geometric approach to rational offsets. *Computer Aided Geometric Design*, 15:223–249, 1998.
- [24] H. Pottmann and M. Peternell. Applications of Laguerre geometry in CAGD. *Computer Aided Geometric Design*, 15:165–186, 1998.
- [25] C. Shene. Blending two cones with Dupin cyclides. *Computer Aided Geometric Design*, 15(7):643–673, 1998.
- [26] K. Shi, J. Yong, J. Sun, and J. Paul.  $G^n$  blending multiple surfaces in polar coordinates. *Computer-Aided Design*, 42:479–494, 2010.
- [27] K. Siddiqi and S. Pizer. *Medial Representations: Mathematics, Algorithms and Applications*. Springer Publishing Company, Incorporated, 1st edition, 2008.
- [28] Q. Song and J. Wang. Generating  $G^n$  parametric blending surfaces based on partial reparameterization of base surfaces. *Computer-Aided Design*, 39:953–963, 2007.
- [29] R. Teixeira. Medial axes and mean curvature motion I: Regular points. *Journal of Visual Communication and Image Representation*, 13(1-2):135 – 155, 2002.
- [30] T. Varady and A. Rockwood. Geometric construction for setback vertex blending. *Computer-Aided Design*, 29:413–425, 1997.
- [31] J. Vida, R. Martin, and T. Varady. A survey of blending methods that use parametric surfaces. *Computer-Aided Design*, 26(5):341–365, 1994.

- [32] J. Wallner and H. Pottmann. Rational blending surfaces between quadrics. *Computer Aided Geometric Design*, 14(5):407–419, 1997.
- [33] J. Warren. Blending algebraic surfaces. *ACM Transactions on Graphics (TOG)*, 8(4):263–278, 1989.
- [34] B. Whited and J. Rossignac. Relative blending. *Computer-Aided Design*, 41:456–462, 2009.
- [35] T. Wu and Y. Zhou. On blending of several quadratic algebraic surfaces. *Computer aided geometric design*, 17(8):759–766, 2000.
- [36] G. Xu. Mixed finite element methods for geometric modeling using general fourth order geometric flows. *Computer Aided Geometric Design*, 26:378–395, 2009.
- [37] P. Yushkevich, P. T. Fletcher, S. Joshi, A. Thall, and S. M. Pizer. Continuous medial representations for geometric object modeling in 2D and 3D. *Image and Vision Computing*, 21(1):17 – 27, 2003.
- [38] P. Zhou and W. Qian. Polyhedral vertex blending with setbacks using rational s-patches. *Computer Aided Geometric Design*, 27:233–244, 2010.
- [39] C. Zhu, R. Wang, X. Shi, and F. Liu. Functional splines with different degrees of smoothness and their applications. *Computer-Aided Design*, 40(5):616–624, 2008.

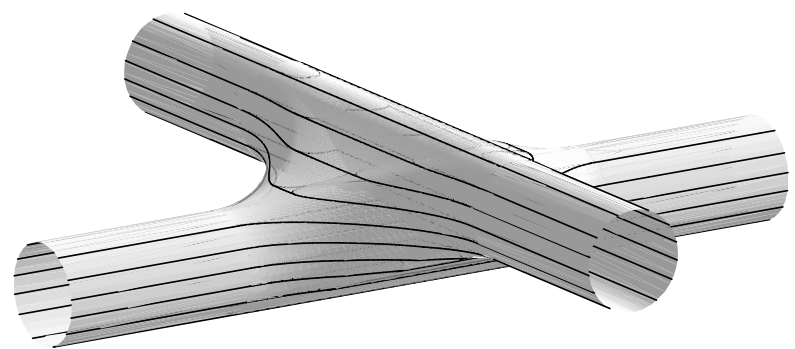
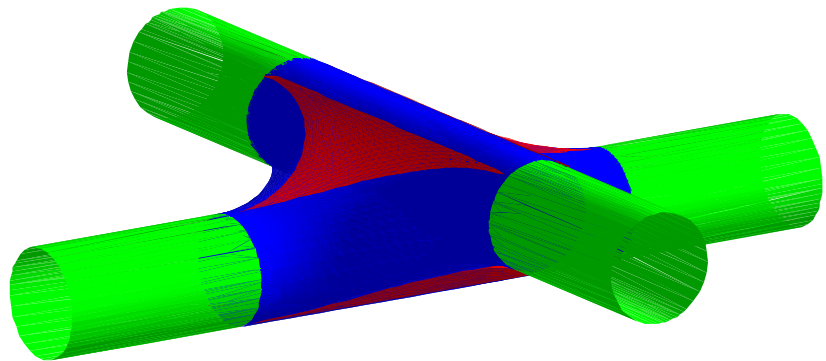
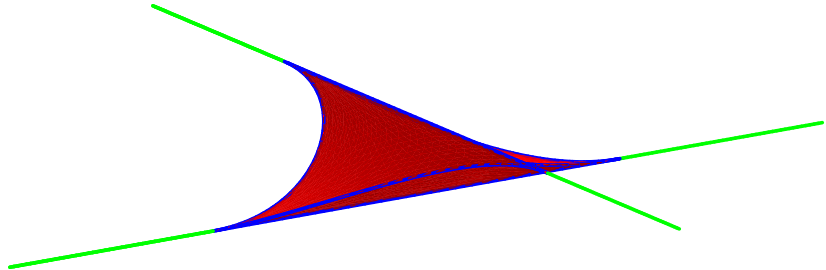


Figure 8: Tetrahedral blend of two cylinders.

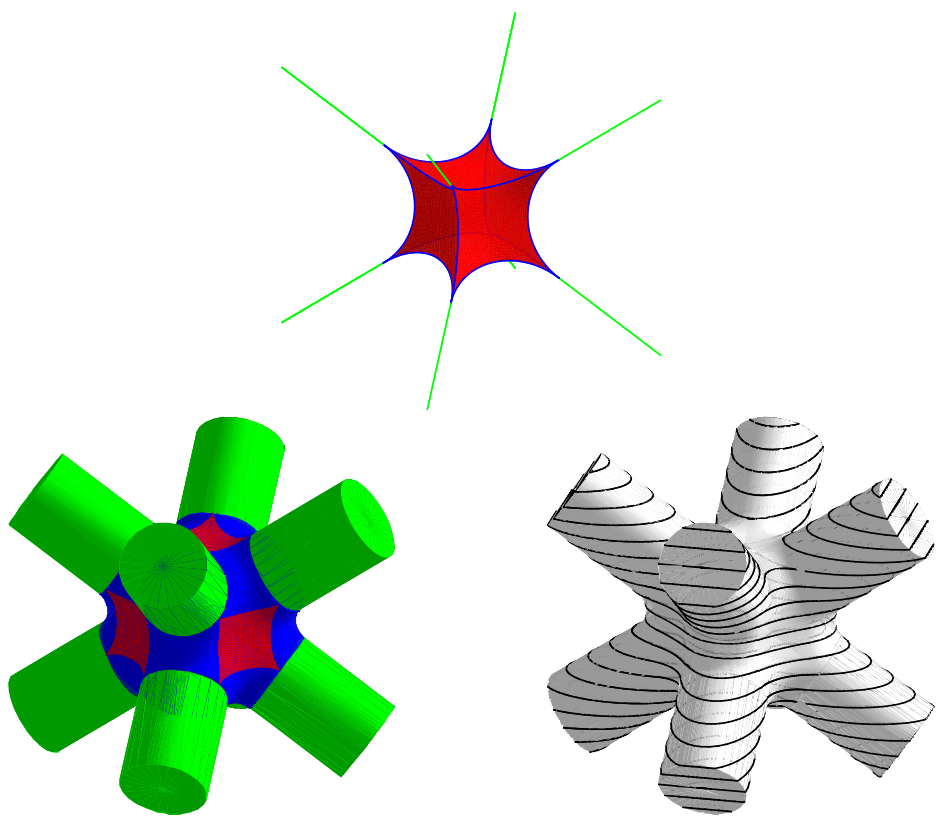


Figure 9: Blend of eight cylinders.

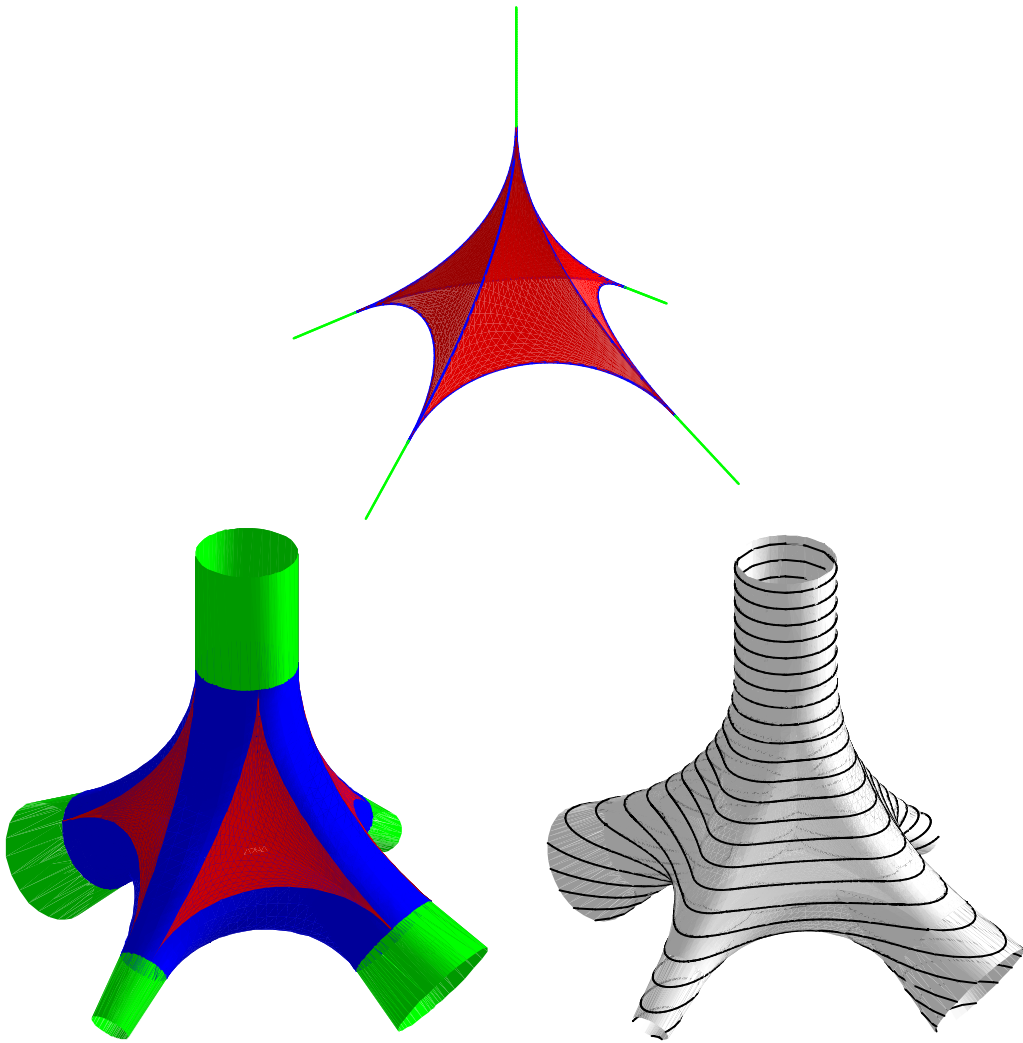


Figure 10: Blend of four cones and a cylinder.